

The phase diagram of bulk nuclear matter

J. B. Elliott, L. G. Moretto, L. Phair and G. J. Wozniak

*Lawrence Berkeley National Laboratory (LBNL)
One Cyclotron Road, Berkeley, CA 94720, USA*

Abstract

Recent analyses of nuclear multifragmentation and compound nuclear data determined the pressure-density-temperature phase diagram of bulk nuclear matter. A condensation model, modified to account for nuclear energies, was used to describe the fragment yields and finite size scaling techniques were used to determine the bulk property of nuclear matter from finite, charged samples of nuclear matter, i.e. nuclei.

1 Introduction

The nuclear thin skin is the basis of the liquid drop model, which reproduces the binding energies of nuclei to within 1%. A similar leptodermous treatment of $T > 0$ nuclear systems should lead to an equivalently good reproduction of nuclear thermodynamical properties, e.g. the liquid-vapor phase diagram.

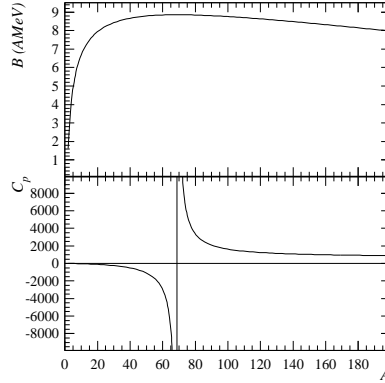
A vapor phase appearing at $T > 0$ opens two complementary perspectives for the characterization of phase coexistence: the liquid and vapor perspectives. From the liquid perspective, one determines the caloric curve in terms of vaporization enthalpy. From the vapor perspective one considers the aggregation of nucleons into clusters, as an indicator of incipient liquid condensation.

In the first section we take the liquid perspective and discuss caloric curves and (negative) heat capacities for drops of nuclear matter. In the second part we take the vapor perspective and show that clusterization in the Ising model is accounted for by a leptodermous expansion. We then apply this perspective to experimental nuclear fragment yields and determine the phase coexistence boundaries of bulk nuclear matter.

2 The liquid path: caloric curves and heat capacities

A decade ago results of several nuclear physics experiments were used to construct a caloric curve [1]. The temperature T from an isotope thermometer was plotted against the excitation energy E^* , resulting in a caloric curve with a rise in T at low E^* , a plateau at moderate E^* and another rise at higher E^* .

This was interpreted as evidence of a first order liquid-vapor phase transition (some controversy surrounded the measurements of T and E^*). However, interpretations of caloric curves depend on the system's pressure p and density ρ . If ρ is constant, caloric curves show a smooth rise in $T(E^*)$. If p is held constant, a constant T with increasing in E^* at coexistence is observed. Neither p nor ρ was known in the experiments used to construct the caloric curve.



The binding energy of atomic nuclei (top) and the associated heat capacity (bottom).

Recently, first order phase transitions in small systems were associated with convex intruders in the entropy S vs. E^* curve resulting in back-bendings in the caloric curve and a negative heat capacity [2]. The claim has been made of an observation of a negative heat capacity in nuclei [3]. For the case of nuclei the specific heat C_p can be calculated directly from the enthalpy ΔH_m , essentially the binding energy $B(A_0, Z_0)$ [4]. When $B(A_0, Z_0)$ decreases with nucleon number A_0 , C_p should be positive. Since the maximum $B(A_0, Z_0)$ occurs at $A_0 \sim 60$, negative C_p values occur only for $A_0 < 60$. Explicitly,

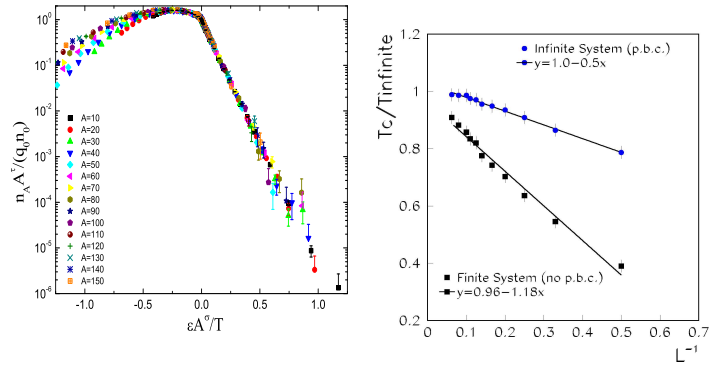
$$C_p = \left. \frac{dH_m}{dT} \right|_p = \frac{[\Delta H_m(A_0)]^2}{T} \bigg/ \frac{d\Delta H_m}{dA_0} = \frac{[\Delta B(A_0, Z_0)]^2}{T} \bigg/ \frac{d\Delta B(A_0, Z_0)}{dA_0}. \quad (1)$$

From Fig. 2 it is clear that $B(A_0, Z_0)$ decreases with A_0 for $A_0 > 60$. Thus in this region of A_0 positive C_p values are expected. Only for $A_0 < 60$ are negative C_p values predicted. This result based on thermodynamics and $B(A_0, Z_0)$ raises questions as to the meaning of the claim of negative heat capacity [3].

3 The (virtual) vapor path: droplet yields

Before taking the vapor path to the nuclear matter phase diagram, we illustrate the way with the Ising model, a simple model with a thermal phase transition

and an established cluster definition. The Hamiltonian of the Ising model, with no external magnetic field, is the interaction between nearest neighbor spins on a fixed lattice $H = -J \sum_{n.n.} s_i s_j$; J is the interaction strength and spins $s_{i,j}$ point up or down. The Ising model is isomorphous with the lattice gas model with up spins as the liquid and down spins acting as the vapor (or vice versa) [5]. Monte Carlo techniques and the Swendsen-Wang algorithm [6] were used to determine equilibrium cluster distribution as a function of T for a simple cubic lattice (lattice side $L = 50$) with periodic boundary conditions and clusters were identified using the Coniglio-Klein [7] formalism [8].



Left: The scaled yields for the $d = 3$ Ising model. Right: Scaling of T_c with lattice side L .

The cluster yields can be described as a function of T and A , the number of spins in a cluster, via Fisher's droplet model [9]

$$n_A(T) = q_0 A^{-\tau} \exp(A \Delta \mu / T) \exp(-c_0 A^\sigma \epsilon / T) \quad (2)$$

q_0 is a normalization constant, τ is a topological exponent, $\Delta \mu$ is the chemical potential distance from coexistence (equal to zero for no external field), c_0 is the surface energy coefficient, σ is the surface to volume exponent and $\epsilon = (T_c - T) / T_c$. A plot of the scaled cluster distributions $n_A(T) / q_0 A^{-\tau}$ as a function of $\epsilon A^\sigma / T$ collapses the data for all cluster sizes onto a line, see Fig. 3, showing that Eq. (2) describes the cluster yields for $T \leq T_c$.

The Ising model also shows how to extrapolate from small to large systems. Finite size scaling is well established [10] and can be understood easily. Considering a finite system (open boundary conditions) a surface is generated with the attendant surface energy allowing us to write a "liquid drop" formula for the Ising model: $B = a_V + a_S A_0^{-1/3}$. All the quantities with the dimension of energy should scale with $B(A_0)$ corrected for the surface energy, thus

$$\frac{T_c(A_0)}{T_c(\infty)} = \frac{B(A_0)}{B(\infty)} = \frac{a_V + a_S A_0^{-1/3}}{a_V} = 1 - \frac{1}{A_0^{1/3}} = 1 - \frac{1}{L} \quad (3)$$

where A_0 is the number of sites. Figure 3 shows this to be the case for the Ising model. T_c for infinite nuclear matter can be obtained in a similar matter.

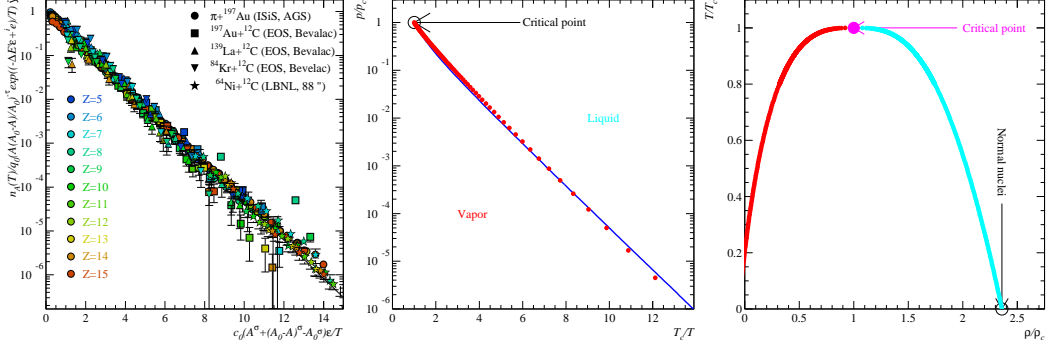
Finally, Fisher's model must be modified to account for the nature of the constituents of the nuclear drops. One begins by assuming, as in a compound nucleus reaction, that the initial collision entity relaxes *quickly* to a thermalized remnant of A_0 nucleons and Z_0 protons, which proceeds *slowly* to emit particles stochastically. The remnant is the liquid evaporating in free space according to standard evaporation theories. In first order phase transitions interaction between the two phases is unnecessary and the rate of evaporation defines the vapor phase, even with no vapor present. The concentration of species A is $n_A(T) = R_A/\bar{v}_A(T)$ where $R_A(T)$ is the emission flux of A and $\bar{v}_A(T)$ is the average velocity of A , $\sim \sqrt{T/A}$. The outward flux, at equilibrium, is the same as the inward flux. Thus, a direct connection is made between the statistical decay rate and Fisher's equilibrium description of cluster formation. Two consequences follow: (i) At equilibrium, the evaporated particle is replaced by back flux from the vapor. However, since the back flux is absent in the case of nuclei, our analysis is limited to particles with low emission probability (first chance). This is achieved by eliminating fragments with $Z < 4$ from our analysis. (ii) The pertinent T is that of the remnant as it evaporates low probability particles. Thus, the Fermi gas relationship $E = aT^2$ is assumed. Returning to We now re-write Fisher's formula as:

$$n_A(T) = q_0 A^{-\tau} \exp\left(\frac{A\Delta\mu}{T}\right) \exp\left(-\frac{\Delta E \varepsilon}{T}\right) \exp\left(\frac{\Delta^I E}{T}\right) \quad (4)$$

where ΔE is the formation energy of a nuclear droplet, depending on $B(A, Z)$ and the Coulomb interaction between the fragment (A, Z) and complement $(A_0 - A, Z_0 - Z)$: $\Delta E = B(A, Z) + B(A_0 - A, Z_0 - A) - B(A_0, Z_0) + E_{Coulomb}(Z, Z_0 - Z)$, with a term for the the angular momentum energy $\Delta^I E = E_{final} - E_{initial}$. Fisher's surface energy term is in ΔE .

The charge yields from the ISiS reaction of 8 GeV/c $\pi + \text{Au}$ [11], the EOS reactions 1.0 AGeV Au+C, 1.0 AGeV La+C and 1.0 AGeV Kr+C [12] and the LBNL 88" reaction $^{64}\text{Ni} + \text{C}$ [13] were fit with Eq. (4). The data in Fig. 3 collapse to a line over six orders of magnitude. The coefficients of $B(A, Z)$ were set to standard values, exponents were set to fluid values (as demanded by universonality [14]). The angular momentum of the fragmentation systems were parameterized individually as linear functions in E^* , the compound nuclear data took a quadratic form; coefficients were fit parameters. The fragment-complement separation r_{sep} was a fit parameter. T was determined via $T = \sqrt{E^*/a}$ where $a = A_0/8(1 + E^*/B(A_0, Z_0))$ accomodates the observed level

density parameter change [15]. The fragment nucleon number A was estimated from the measured fragment charge Z via $A = 2Z(1 + yE^*/B(A, Z))$ where the factor in parenthesis accounts for secondary decay, y is a fit parameter. $T_c(A_0, Z_0)$ was determined via Eq. (3) with $T_c(\infty)$ as a fit parameter. The fragmentation systems' angular momenta were $\sim 20\hbar$, the compound nuclear system angular momentum was close to previous estimates [13], $r_{sep} = 5.0 \pm 0.1$ fm, $y = 0.33 \pm 0.01$ close previous estimates [16] and $T_c(\infty) = 15.7 \pm 0.2$ MeV.



Left: The scaled yields for five different nuclear data sets. Middle: The p - T coexistence line. Right: The T - ρ coexistence curve. Both for bulk nuclear matter.

By noting that Fisher's model assumes a non-ideal vapor can be approximated by an ideal gas of clusters and using the values of the parameters above, the coexistence curve observed in the scaled fragment yields in Fig. 3 can be cast into a more familiar form. The quantity n_A is proportional to the partial pressure of a fragment of mass A and the total pressure is the sum of the partial pressures: $p = T \sum n_A$. The reduced pressure is given by $p/p_c = T \sum n_A(T) / T_c \sum n_A(T_c)$. The coexistence line for bulk nuclear matter is then obtained by using $n_A(T, \Delta\mu = 0, E_{Coulomb} = 0, E_{symmetry})$ from Eq. (4). See Fig. 3. Recalling the Clausius-Clapeyron equation: $dp/dT = \Delta H / T \Delta V$ one obtains: $p/p_c = \exp(\Delta H / T_c (1 - T_c/T))$ which describes several fluids up to T_c [17]. Fitting the coexistence line and using the above value of T_c and $\Delta H = \Delta E - pV$ with $pV = T$ gives a value for $\Delta E \approx 15.8$ MeV, close to the bulk energy coefficient. The system's density is $\rho = \sum A n_A$, and the reduced density from $\rho/\rho_c = \sum A n_A(T) / \sum A n_A(T_c)$. The vapor branch of the coexistence curve is found by setting all energies other than surface to zero for $n_A(T)$ in Eq. (4). See Fig. 3. It is possible to determine the liquid branch as well: empirically $\rho_{coex}/\rho_c - T/T_c$ for several fluids can be fit with the function $\rho_{l,v}/\rho_c = 1 + b_1(1 - T/T_c) \pm b_2(1 - T/T_c)^{1/3}$ [17], where b_2 is positive (negative) for the liquid (ρ_l) (vapor ρ_v) branch. It was later recognized that the power of $1/3$ was the critical exponent β . Using Fisher's model, β can be determined

from τ and σ : $\beta = (\tau - 2)/\sigma = (2.21 - 2)/0.64 = 0.31$. Fitting the vapor branch of the coexistence curve gives and changing the sign of b_2 gives the liquid branch of the coexistence curve. If normal nuclei exist at the $T = 0$ point of the coexistence curve, then $\rho_c \sim 0.42\rho_0$. The critical compressibility factor $C_c^F = p_c/T_c\rho_c$, found via the appropriate sums, is ~ 0.29 , in agreement with the values for several fluids [18]. Using T_c and ρ_c from above in combination with C_c^F gives a critical pressure of $p_c \sim 0.3 \text{ MeV / fm}^3$.

4 Acknowledgments

We thank Prof. C.M. Mader, Prof. R. Ghatti and Prof. J. Helgesson for their input and Ising calculations and acknowledge the efforts of the ISiS and EOS collaborations. This work was supported by the U.S. Department of Energy.

References

- [1] J. Pochodzalla, *et al.*, Phys. Rev. Lett. **75**, 1040 (1995).
- [2] D.H.E. Gross, Phys. Rep. **279**, 119 (1997).
- [3] M.D'Agostino *et al.*, Phys. Lett. B, **473**, 219 (2000).
- [4] L.G. Moretto, Phys. Rev. C **66**, 041601(R) (2002).
- [5] T.D. Lee and C. N. Yang, Phys. Rev. **87**, 404 (1952).
- [6] J. S. Wang and R. H. Swendsen, Physica A **167**, 565 (1990).
- [7] A. Coniglio and W. Klein, J. Phys. A **13**, 2775 (1980).
- [8] C.M. Mader *et al.*, LBNL-47575, nucl-th/0103030 (2001).
- [9] M.E. Fisher, Physics **3**, 255 (1967).
- [10] M.E. Fisher and A. E. Ferdinand, Phys. Rev. Lett. **19**, 169 (1967).
- [11] L. Beaulieu *et al.*, Phys. Rev. C **63**, 031302 (2001).
- [12] J.A. Hauger *et al.*, Phys. Rev. C **62**, 024626 (2000).
- [13] T.S. Fan, *et al.*, Nucl. Phys. A **679**, 121 (2000).
- [14] J.M. Yeomans, "Stat. Mech. of Phase Transitions", (Oxford, 1992).
- [15] K. Hagel *et al.*, Nucl. Phys. **A486**, 429 (1988).
- [16] J. B. Elliott *et al.*, Phys. Rev. C (2003).
- [17] E.A. Guggenheim, "Thermodynamics", 4th ed. (North-Holland, 1993).
- [18] C. S. Kiang, Phys. Rev. Lett. **24**, 47 (1970).